

Reprinted from

**Symposium on**

**Machine Processing of**

**Remotely Sensed Data**

**June 29 - July 1, 1976**

The Laboratory for Applications of  
Remote Sensing

Purdue University  
West Lafayette  
Indiana

IEEE Catalog No.  
76CH1103-1 MPRSD

Copyright © 1976 IEEE  
The Institute of Electrical and Electronics Engineers, Inc.

Copyright © 2004 IEEE. This material is provided with permission of the IEEE. Such permission of the IEEE does not in any way imply IEEE endorsement of any of the products or services of the Purdue Research Foundation/University. Internal or personal use of this material is permitted. However, permission to reprint/republish this material for advertising or promotional purposes or for creating new collective works for resale or redistribution must be obtained from the IEEE by writing to [pubs-permissions@ieee.org](mailto:pubs-permissions@ieee.org).

By choosing to view this document, you agree to all provisions of the copyright laws protecting it.

THE TASSELLED CAP -- A GRAPHIC DESCRIPTION OF THE SPECTRAL-TEMPORAL  
DEVELOPMENT OF AGRICULTURAL CROPS AS SEEN BY LANDSAT\*

R. J. Kauth and G. S. Thomas

Environmental Research Institute of Michigan  
Ann Arbor, Michigan

I. ABSTRACT

The time trajectories of agricultural data points as seen in LANDSAT signal space form a pattern suggestive of a tasselled woolly cap. Using this easily visualized three dimensional construct most of the important phenomena of crop development and observation variables are pointed out, named, discussed and measured. The important crop phenomena described are the distribution of signals from bare soil, the processes of green development, of yellow development, of shadowing and of harvesting. The important external variables include view angle, sun angle, atmospheric haze, and atmospheric water vapor.

The development of a quantitative picture of the tasselled cap depends upon crop and atmosphere effects modeling and upon empirical observation of data signals. Quantitative data from a composite of these sources is given. The tasselled cap structure is illustrated with cluster plots and diagrams.

The tasselled cap is a fertile source of ideas for processing techniques. Examples discussed include

- a) A linear preprocessing transformation which isolates green development, yellow development and soil brightness and allows the reduction of the dimension of the feature space.
- b) The use of specific measurable pattern elements of the tasselled cap structure to estimate and correct atmospheric haze and moisture effects.

II. INTRODUCTION

The problem is to be able to identify some agricultural crop systematically on a large scale, based on remotely sensed data acquired at a number of times. The pattern of the particular crop must be distinguished from the patterns of multiple other crops which may or may not always be present. Multi-

farious external effects influence the pattern of the crop in question as well as the pattern of all other crops. The number of variables is very large. In this environment how do we proceed in the design of a processor?

The first step is to find a variety of ways to display the data. Given the displays, one will notice the structure of the data, will name the data structures, will create some visual model of the data structure. Such a model may suggest a physical interpretation or a quantitative test. One then subjects the description to quantitative tests, resulting in gradual elaboration and refinement of the description, or, in some cases, resulting in its destruction.

Let us proceed then to look at the structure of LANDSAT data of agricultural crops, leading to the visual model of the tasselled cap.

III. THE TASSELLED CAP

Figure 1(a) shows a two channel scatter diagram of LANDSAT data in an agricultural scene in Fayette Co., Illinois. The data has been compressed by unsupervised spectral clustering of the data points in all 4 LANDSAT MSS channels. The ellipses shown are the unit contour ellipses of the normal density function describing each cluster. The channels shown are CH 2 and CH 3.

Notice in Figure 1(a) the definite boundary region near the diagonal of the two channel presentation. All of the agricultural data lies to the left of this boundary. To the right of the boundary there is no data. The region to the left shows a definite triangle like shape, with two vertices on the diagonal and one near the CH 3 axis.

Figure 1(b) shows a similar cluster plot of CH 1 vs. CH 2. Here, all of the data lies near a diagonal of the space again. Thus we can infer that the triangle shaped region of Figure 1(a) is shown edge on in Figure 1(b). The three-dimensional shape

---

\* The effort described herein was supported by the Earth Observations Division of the NASA/Johnson Space Center under Contract NAS9-14123.

of the data structure is that of a flattened triangular shape having little thickness. Figure 1(c) shows a cluster plot of CH 3 vs. CH 4. Again the data lies closely along a diagonal. Viewing only Figures 1(a) and 1(c), one would conclude that, seen in the 3 space of Channels 2, 3 and 4 the three-dimensional shape of the data structure is a flattened triangular shape. One then can conclude that the data structure forms a flattened triangular shape in 4 dimensions, and that is correct.

Figures 1(d), 1(e) and 1(f) show the same data in channel pairs 1 vs. 3, 2 vs. 4 and 1 vs. 4. If one assumes that CH 1 is highly correlated to CH 2 (as it seems to be, based on Figure 1(b)) and that CH 4 is highly correlated to CH 3 (as it seems to be, based on Figure 1(c)), then these last 3 figures offer no particular surprises; they are in a manner of speaking first and second cousins of Figure 1(a). (The fact of the high correlation of CH 1 with CH 2 and of CH 4 with CH 3 has sometimes stimulated the comment that LANDSAT MSS is essentially a two channel system; that no information would be lost by throwing away CH 1 and CH 4. On the contrary, there is significant information of several types contained in the 4 channels, as we shall see as this discussion develops.)

What is the physical reason for the data to lie in this flattened triangular structure? Figure 2 shows a model calculation of the reflectance of a crop canopy at two wavelengths, .65 nm and .75 nm, corresponding to the centers of CH 2 and CH 3. The calculations were made for two soil samples, one dark, the other light, through the life of the crop. Notably, the triangular shape is outlined by the two crop life development lines. After the crop canopy cover the soil completely the two canopies look identical. Figure 2 is extracted from Reference 1. The canopy model used was developed by G. Suits<sup>2</sup>. Roughly what seems to be occurring is that the crop starts its growth on the line of soils. As it grows the composite reflectance of soil and crop increases in CH 3 because of the presence of cellulose in the plant. The composite reflectance of CH 2 decreases because of the chlorophyll in the plants is highly absorbing. Hence the radiance typical of green plants is located to the left, at the tip of the triangle.

Figure 2 attempts to span the range of soil conditions by the terms "light" and "dark". Is this all there is to soils as seen in LANDSAT data? Condit<sup>3,4</sup> has measured the spectral reflectance of soil samples from all over the United States, and analyzed them in terms of their principal spectral components. We have used Condit's data to calculate the soil distribution that would be seen by the LANDSAT MSS spectral filters. Table 1 shows the soil reflectance mean vector and principal components in LANDSAT data. We will summarize those results in the following discussion.

Figure 3 gives an idea of the distribution of soil reflectances projected into the 4 dimensions spanned by the 4 LANDSAT MSS channels. That space has a "diagonal", i.e., a line along which the normalized reflectance of all channels is equal. The mean reflectance of soils lies near that diagonal.

The largest principal component of soil reflectance is nearly parallel to the diagonal. The square root of the eigenvalue associated with the first component is about 35 units, (i.e., one standard deviation of the data projected onto the first principal component is about 35). The second principal component, normal to the first, has a standard deviation of about 5 units the third of about 3 units and the fourth of about 1 1/2 units. The unit contour ellipsoid describing the distribution of soils forms a four dimensional flattened cigar shape, about seven times as long as it is wide, about twice as wide as it is thick, and twice as thick as it is thin (what is the name for distance in the 4<sup>th</sup> direction?). Hence, for some applications we would be justified in describing the data from soil points as the "line of soils", ignoring all but the major component. In other cases we might speak of the "plane of soils", referring to the first and second component.

Returning now to Figure 2, we notice again that after the initial development stages the two crop canopy trajectories join and fall back towards the soil line. What cannot be seen in this figure is that the line of falling back is not in the same plane (in the 4 space of LANDSAT data) as the two development lines up to the point of joining. The crop is yellowing, and yellow colored things lie in a different direction away from the soil line than do green colored things.

We now have sufficient information to create the basic image of the tasselled cap, shown in Figure 4.

The basic tasselled cap shown in Figure 4 is created by combining soil reflectance and green stuff and then adding yellow stuff. We say that the crop starts growing on the plane of soils. As it grows it progresses outward, roughly normal to the plane of soils, on a curving trajectory towards the region of green stuff. Next the trajectories fold over and converge on the region of yellow stuff. Finally the crop progresses back to the soil from whence it came (dust from dust?) by any of several routes, depending on the crop and the harvesting practices.

Initially we spoke of a flattened triangle, now we are likening the data structure to a tasselled cap. To fit both of these images the yellow point must be quite close to the side of the cap, and indeed that is true. For wheat the yellow is also accompanied by shadowing so that the yellow point is found near the dark end of the plane of soils.

The "front" of the cap looks down toward the origin of all data otherwise called THE ORIGIN. On the front of the cap is the badge of trees. Why the reflectance of trees is located just here will be explained a little further on.

#### Effects of Shadow

As the crop canopy develops away from the soil the average reflectance becomes more green, but at the same time shadows develop. Initially, much of this shadow will appear on the soil portions of the

composite canopy. Thus the reflectance of a crop planted on bright soil will initially migrate mainly in the direction of the origin.

A crop which is planted on dark soil will not show this behavior significantly. After all there is little difference between the radiance of dark soil and the radiance of shadowed dark soil.

Once maximum shadowing on the soil has been reached the reflectance is more strongly influenced by the addition of green elements to the canopy. Thus the trajectory of reflectance values sweeps away from the plane of soils. Initially many of the green elements that are added are shadowed green elements. Hence the total reflectance remains low until most of the ground is covered.

In the next stage the canopy loses most of its shadows, reaching a state of full green development. Whether a crop actually reaches this stage depends upon the planting density and upon the way its leaves form together to make a canopy.

This curving trajectory has been documented by F. Johnson<sup>5</sup> in Fayette County corn field data, and also has been shown in the results of a detailed modelling exercise being presented at this symposium<sup>6</sup>. Interestingly, Johnson has found that corn planted in East-West rows does not show this behavior significantly, whilst corn planted in North-South rows does show a very strong shadow effect. The reason is clear. At the time of the LANDSAT overpass the Sun's rays are coming mainly from the east. Sunlight falls down the East-West rows and shadows fall on the sides of other corn plants rather than in the open rows.

Now we can see why trees occupy the place they do in reflectance space. Trees are green canopies structured so as to create a good deal of shadow.

#### IV. A FIXED LINEAR TRANSFORMATION

It is difficult to look at LANDSAT data and see all of the features so far described. After all, this is a 4-dimensional space we are looking at, and it is hard to be sure we are seeing everything. Therefore we have developed some transformations of the data which assist us to see it better.\* The only one of these we will discuss at this point is a fixed affine transformation,

$$u = R^T x + r \quad (1)$$

where

$x$  is the LANDSAT MSS signal vector expressed in counts

$u$  is the transformed vector, also expressed in counts

$r$  is an offset vector, introduced to avoid negative values in the transformed data

$R$  is a unitary matrix, i.e., the columns of  $R$  are unit vectors  $R_1, R_2, R_3$  and  $R_4$ , which are all orthogonal to each other. Superscript  $T$  indicates the transpose. Thus the application of the transformation to the data  $x$  results in a pure rotation plus a pure translation.

The components of  $R$  are chosen in the following way:

$R_1$  is chosen to point along the major axis of soils, in the LANDSAT data. A particular sample of LANDSAT data was chosen to derive  $R_1$ , namely Fayette County, Illinois, June 1973. Visual inspection of Figure 1(a) was used to pick out 12 soil line clusters. The best fit line to those 12 clusters was chosen as the direction of  $R_1$ .  $R_1$  is called the soil brightness unit vector. The projection of a data point onto  $R_1$  is a feature called brightness.

$R_2$  is chosen to point orthogonal to  $R_1$  and toward a green cluster in the same data set. Visual inspection of Figure 1 was used to identify the cluster.  $R_2$  was generated using the Gram-Schmidt orthogonalization procedure.  $R_2$  is the green stuff unit vector. The projection of a data point onto  $R_2$  is a feature called "green stuff".

$R_3$  is chosen orthogonal to both  $R_1$  and  $R_2$  and points toward a yellow stuff point. There was no yellow stuff in the Fayette segment, hence an approximate spectrum of yellow corn was used to simulate or predict the yellow point in the Fayette data. Again the Gram-Schmidt procedure was used to derive the yellow stuff unit vector.

$R_4$  is chosen orthogonal to  $R_1, R_2$  and  $R_3$ . The projection of a data point onto  $R_4$  is a feature called "non-such".

The values for  $R_1, R_2, R_3$  and  $R_4$  are, to the third decimal place,

$$R_1 = \begin{pmatrix} .433 \\ .632 \\ .586 \\ .264 \end{pmatrix} \quad R_2 = \begin{pmatrix} -.290 \\ -.562 \\ .600 \\ .491 \end{pmatrix}$$

$$R_3 = \begin{pmatrix} -.829 \\ .522 \\ -.039 \\ .194 \end{pmatrix} \quad R_4 = \begin{pmatrix} .223 \\ .012 \\ -.543 \\ .810 \end{pmatrix}$$

The offset vector is arbitrary. All components equal to 32 seems to work well.

\* The transformations we have developed have depended in part on the work of F. Johnson.<sup>5</sup>

The fixed linear transformation has several potential uses.

a) Simply by projecting the clustered data in terms of the features of Equation 1 we can see the data structure easily. We can also examine it to determine to what extent it actually behaves according to our imaginary picture.

b) Potentially there is significantly less information in some of the transformed channels than in others, whereas each of the original channels is about equally information carrying. Thus one might be able to ignore certain of the transformed channels and this could lead to cost reduction in processing.

c) The transformation of the data allows certain diagnostic features to be extracted which are symptomatic of external effects, such as haze,  $H_2O$  vapor, illumination angle and viewing angle.

In order to picture the data resulting from the fixed linear transformation we show Figures 5(a) through 5(f), which are cluster plots of the data presented in the pairs of transformed channels. The data shown is from the Ellis Co. ITS, dated June 13, 1973. (Recall that the transformation was developed on Illinois data.) Notice that transformed channel 1, (TCH 1), which is soil brightness, and TCH 2, green stuff, contain almost all of the variation within the sample segment.

Figure 5(a) shows these two channels plotted against each other. The basic triangle shape is easily noted, now rotated to the right so that the soil line is parallel with the soil brightness axis. One noticeable effect of the transformation is to increase the apparent size of the tasselled cap, even though there was not any scale factor built in to the transformation. The reason is that in the transformed data we are seeing the tasselled cap directly from the side.

Figure 5(b) shows the yellow feature plotted versus the green feature. Notice that the data is greatly compressed in the yellow direction. There are a few small clusters to the side of the main group of clusters, which are, perhaps, examples of yellow materials.

Figure 5(c) shows non-such versus brightness. There is evidently no structure at all in the non-such direction. Figure 5(f) shows non-such versus yellow stuff. One could easily believe that these channels together carry only a tiny fraction of the information available in LANDSAT data. However, yellow stuff does show definite spatial structure at some times, as we will see later.

A second method of presentation of transformed data is by viewing transformed imagery. Figure 6 shows green stuff images of a LACIE sample segment in Kansas, during 4 successive biophases.\* The region at the top and bottom of the segment contains

numerous winter wheat fields. The region at the center is rangeland. Figure 7 is the soil brightness image of the same data. Figure 8(b) shows non-such in the 4<sup>th</sup> biophase and is reasonably typical of non-such and yellow stuff in all of the biophases, i.e., mainly noise with almost no discernible structure. Figure 8(a) is yellow stuff in the 4<sup>th</sup> biophase. Although the dynamic range of the data is only about 10 counts, which is comparable to Figure 8(b), the strong spatial structure is evident.

Returning to Figure 6(a), we note the rangeland is somewhat green, but the fields are not green at all. The roads show up, if at all, as slightly green, due to the grass on the roadside. In Figure 6(b), the second biophase, the fields show up strongly green, while the rangeland is still only somewhat green. In Figure 6(c), the third biophase, both rangeland and winter wheat are green; one can imagine that the rangeland has caught up with the wheat. Finally in Figure 6(d), the 4<sup>th</sup> biophase, the wheat is again not green.

Returning to Figure 7(a), we see the soil brightness during the first biophase. One striking affect is the way the roads stand out in this image. Notice that the wheat fields are generally, but not entirely, dark. Basically these are bare soil fields and we could expect some to be light and some dark.

In Figure 7(b) the wheat fields are dark; we interpret this to mean that the fields have developed shadow in them in the process of growing. The rangeland is substantially unchanged between biophases 1 and 2, in the soil brightness feature. The roads are still bright.

In Figure 7(c), the 3<sup>rd</sup> biophase, the wheat fields have brightened up, as has the rangeland. There is little contrast between the two.

In Figure 7(d), the 4<sup>th</sup> biophase, some of the wheat fields are bright, others are not. We interpret this to mean that some are harvested (no shadows) and others are not harvested. Notice that all of the areas that appear to be wheat are yellow in the 4<sup>th</sup> biophase, but only some are bright (see Figure 8(a)). In the 4<sup>th</sup> biophase the rangeland is again moderately bright. The roads stand out by bright contrast.

Earlier we commented that there was more than two channels worth of information contained in LANDSAT data. Here we have shown an example. The green feature, the yellow feature, and the brightness feature are three independent measurements. They could not all be measured and represented by a two channel LANDSAT.

A third method of viewing transformed data is by looking at tables of cluster statistics or training statistics. This approach is utilized in the discussion in the following section.

\* Q. Holmes, NASA/JSC, transformed the data used in this and the next example, and created the imagery we have used in Figures 6 through 8.

## V. THE PROBLEM OF CORRECTION FOR EXTERNAL EFFECTS

We have discussed the Tasselled Cap as a way of integrating the spectral reflectance structure of a LANDSAT MSS agricultural scene. The reflectance has, for some specified conditions of observation, a corresponding radiance and a corresponding representation in LANDSAT counts. As the conditions of observation change, however, the relationship between reflectance and LANDSAT counts changes. By observation conditions we mean such items as the viewing and illumination geometry, the amount of haze in the atmosphere, the amount of H<sub>2</sub>O vapor, the amount of cirrus cloud and the height distribution of these in the atmosphere; also the average ground albedo in the neighborhood of the particular observed points.

Some combination of these effects is without doubt extremely significant to the problem of identifying field types in LANDSAT data. The very fact that the data within a local area is confined to an extremely flattened structure within the LANDSAT signal space makes it easier in a certain sense to make errors in classification. Figure 9 shows a hypothetical two-channel example in which external effects (haze perhaps) can shift the entire data collection sideways. Two crops, W and V, occupy a narrow region of the space, and are easily separable in that region. Assume that we train a classifier on the data from one sample segment, obtaining the signatures W and V. Then assume that the conditions change and the entire region shifts to the position represented by W' and V'. Classification errors will now occur, but more than that, there will be a great deal of thresholding. In fact Figure 9 represents quite well what really occurs due to the addition of haze to the atmosphere over a scene. The equivalent occurrence in the 4-dimensional case of LANDSAT data would consist of a shift of the entire tasselled cap in the yellow stuff or non-such direction. Such shifts, ranging up to several standard deviations of the yellow stuff channel have been observed in randomly selected LACIE sample segments in Kansas (where standard deviation refers to the thickness of the entire tasselled cap in the yellow stuff direction).

Figure 9 also shows a shift in the brightness direction. In the real case a negative shift in the yellow stuff direction due to haze is also accompanied by a positive shift in brightness and a negative shift in greenness, as well as a general contraction in scale (i.e., loss of contrast). The interactions are complicated and outside the scope of this paper. The key point is that the yellow shift and the non-such shift are diagnostic of a physical state of the atmosphere. We are attempting to exploit these diagnostic features for purposes of correcting the data for the effects of haze and viewing angle<sup>7,8</sup>.

Imagine now that a cloud represents an extreme case of haze. Then, according to the relationships suggested in the previous paragraph, a cloud would appear extremely shifted in both the negative yellow stuff and the positive brightness direction. We

are experimenting with a cloud detector based on this idea, i.e., if the quantity  $u_1 - u_3$  passes a certain threshold a pixel is labeled cloud. ( $u_1$  and  $u_3$  are the brightness and yellow stuff components of the vector  $u$  shown in Equation 1.)

## VI. POINT OF ALL SHADOW

Figure 4 shows a feature, a point located somewhere back of the origin, called the point of all shadow (see also Appendix B). As we change viewing angle and illumination angle the amount of shadow which can be seen in the canopy varies. The reflectance of the canopy therefore changes, becoming lighter or darker. However, the changes are not merely towards or away from the origin, as they would be if only a change in illumination level were involved; there is also a color shift, since the radiation reflected from within the shadow region is more strongly colored than that reflected from the unshadowed region.

By making a shift of coordinates to the point of all shadow the data can be treated as though the changes in illumination and viewing angles did not induce any color shift, but only a brightness change.

The key idea about the point of all shadow is that all points lying on any radius from this point are at the same stage of crop development. This is no doubt not perfectly true -- it is in fact only an idea. But a slightly simpler version of this same idea forms the basis for the red to infrared ratio (i.e., CH 3 divided by CH 2) as a measure of green biomass<sup>7</sup>.

To be specific, we propose to use a transformation of the form

$$v = Q^T \frac{(x - \beta)}{s} + r \quad (2)$$

where

$x$  is the LANDSAT signal vector after haze correction

$\beta$  is the point of all shadow

$s$  is a brightness measure

$$\left( \text{e.g., } \sum_{i=1}^4 (x_i - \beta_i) = s \right)$$

$Q^T$  is a dimension reducing matrix such that,

$$v = \begin{pmatrix} v_1 \\ v_2 \end{pmatrix} = \begin{pmatrix} \text{green color feature} \\ \text{yellow color feature} \end{pmatrix}$$

Thus three features would be retained for processing --  $s$  and the two components of  $v$ .

In order to use this idea we have to pick a point of all shadow to work with. Several comments are in order:

a) The point of all shadow should be chosen on the extended line of soils, even if that is not truly on the reflectance diagonal. In this way natural soil brightness variation will be lumped together with shadow variation.

b) We can pick a working shadow point and use it. If we have some success, then systematic efforts should be made to establish its position more accurately.

c) The point of all shadow will be modified by atmosphere (haze) effects in the same way that any other point in the reflectance space will be. Any transformed features which utilize the point of all shadow as an origin will be dependent upon the haze level. Therefore it will be necessary to carry out a correction for haze in order to properly exploit the color feature representation.

### VII. SUMMARY

The purpose of this paper is to illustrate the usefulness of obtaining insight and understanding of the overall data structure in a pictorial/geometric sense. Introducing precise but colorful language is useful because it allows groups of workers to communicate their developing ideas in a graphic shorthand manner.

The following summary statements can be made:

a) The data from an agricultural scene lies substantially on a plane in LANDSAT signal space, spanned by brightness and green development, except that some protrusions out of the plane in a yellow direction are observable.

b) Within the plane the data are bounded in a triangular region.

c) The position of the entire plane and the boundaries within it are indicative of the external conditions of observation and can be used to estimate those conditions.

d) A fixed linear transform can be used to aid in viewing the data and to create diagnostic features from the data.

e) The primary description of agricultural crops is in their color and brightness -- non-linear functions of the LANDSAT channels. A transformation to a color-brightness feature space is suggested. Haze correction should be accomplished prior to application of the non-linear transformation.

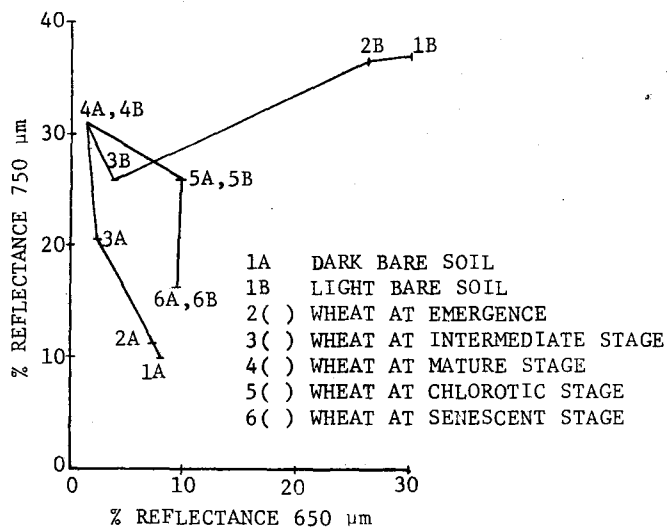


Figure 2. Phenology for Wheat (Ionia Variety) Based on Canopy Model

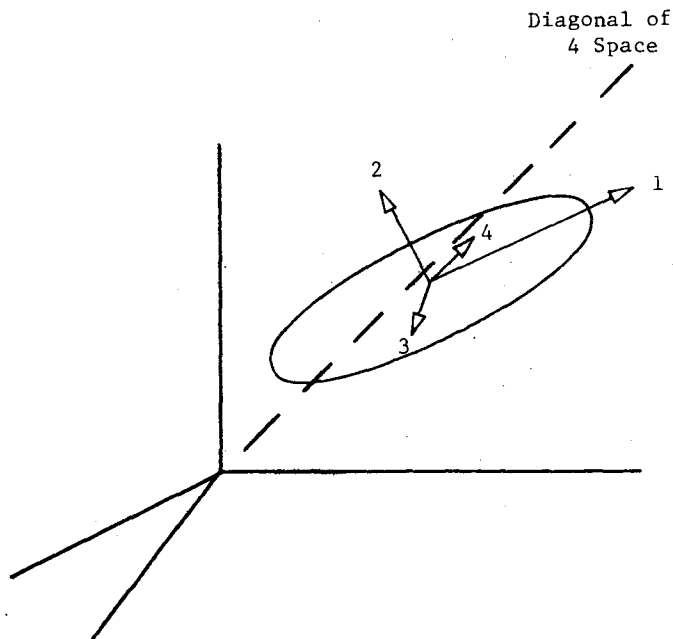


Figure 3. Concept of Soil Distribution in 4-Dimensions

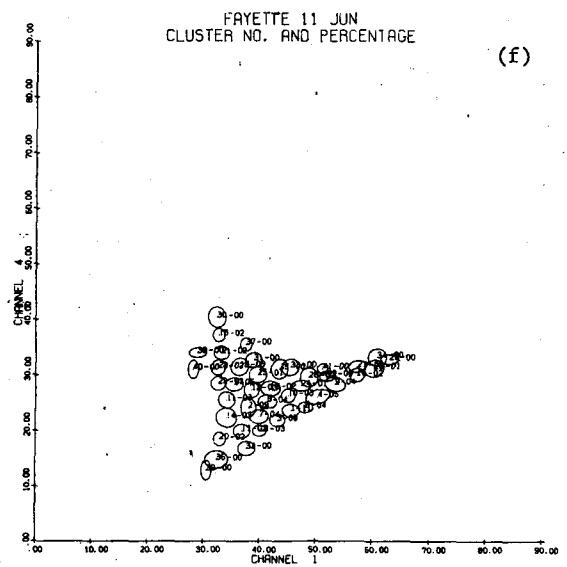
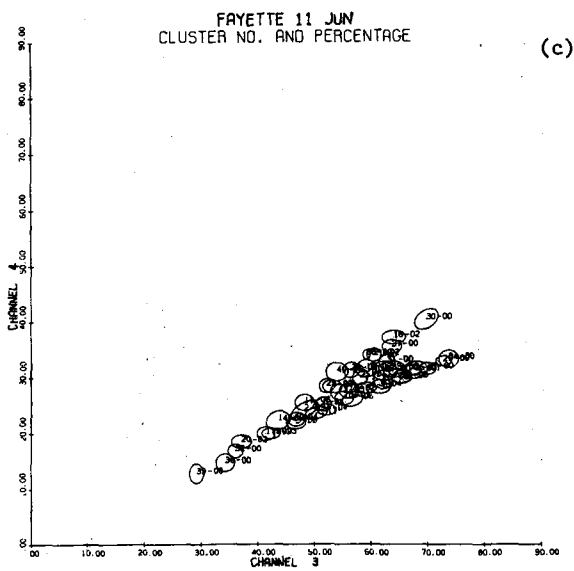
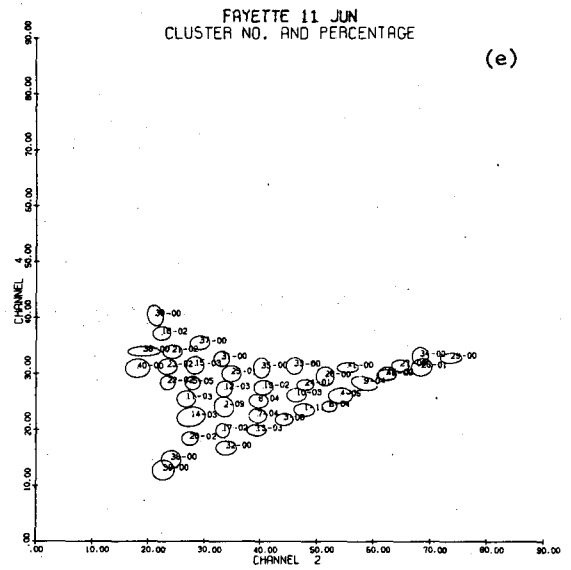
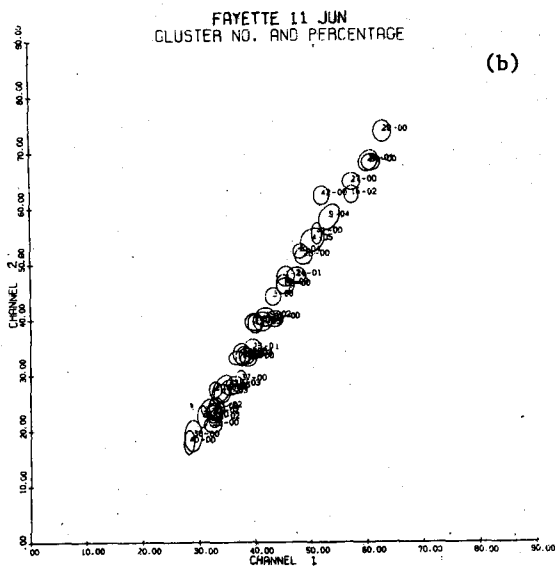
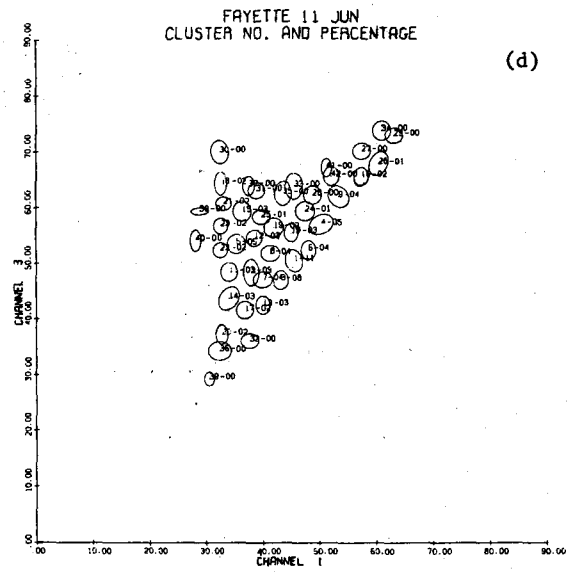
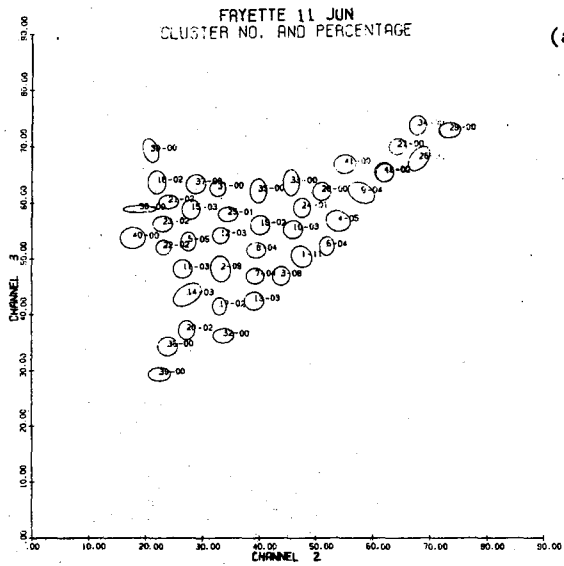


Figure 1. Unsupervised Cluster Plots, Fayette Co., Illinois



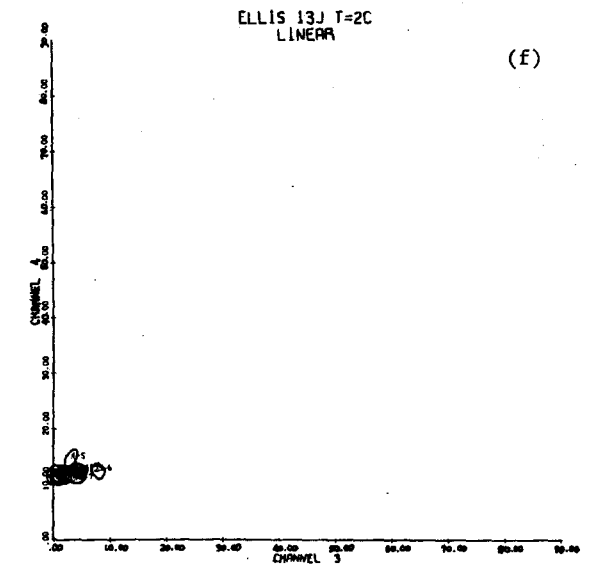
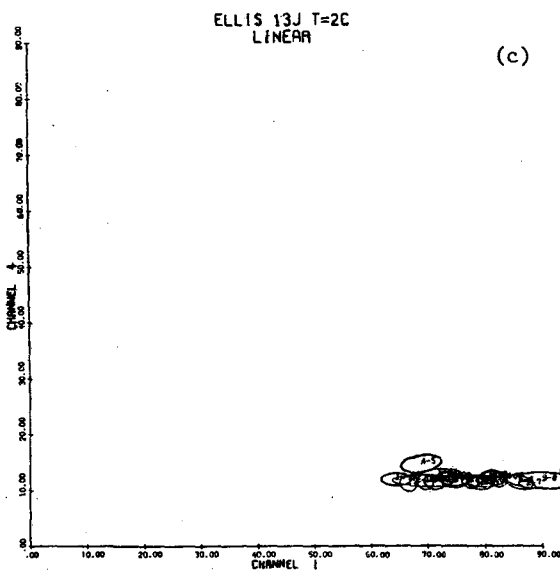
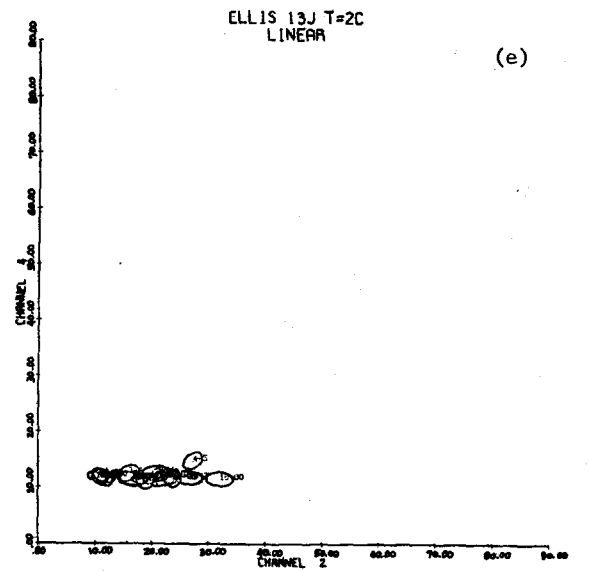
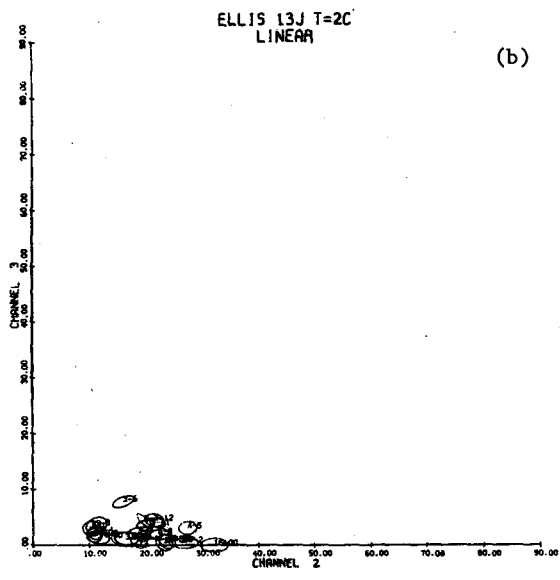
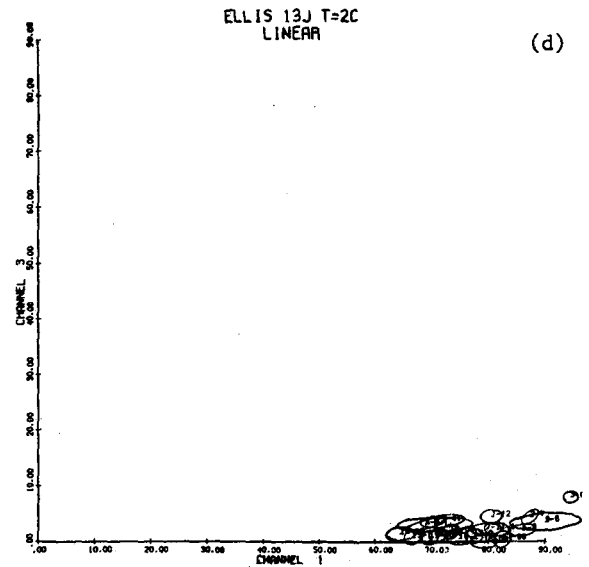
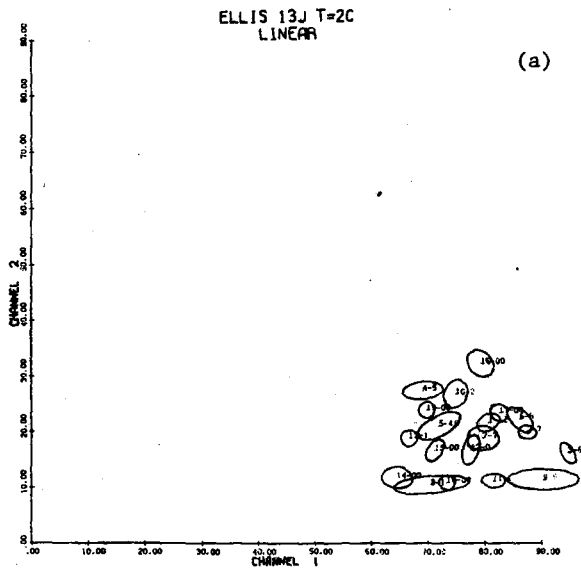


Figure 5. Cluster Plots of Linearly Transformed Data, Ellis Co., Illinois

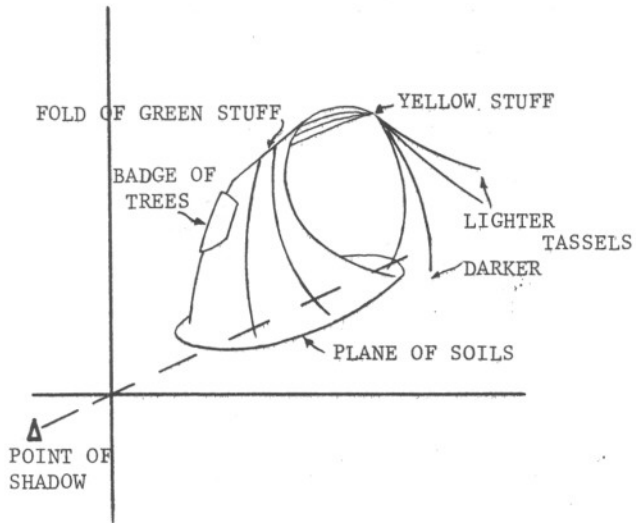
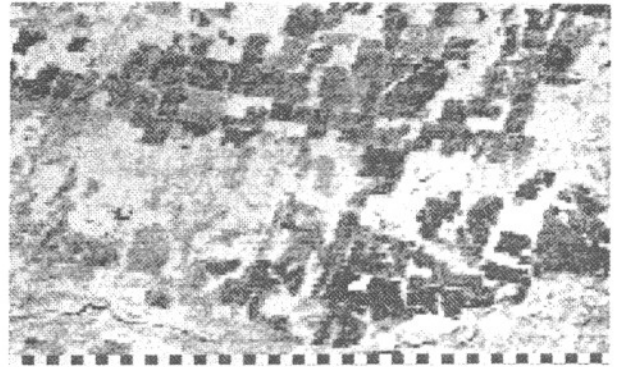
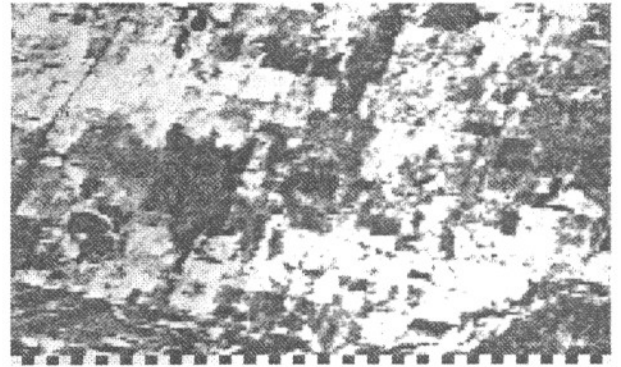


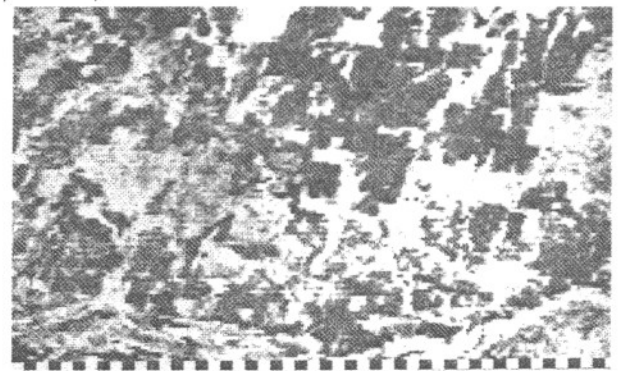
Figure 4. The Tasselled Cap



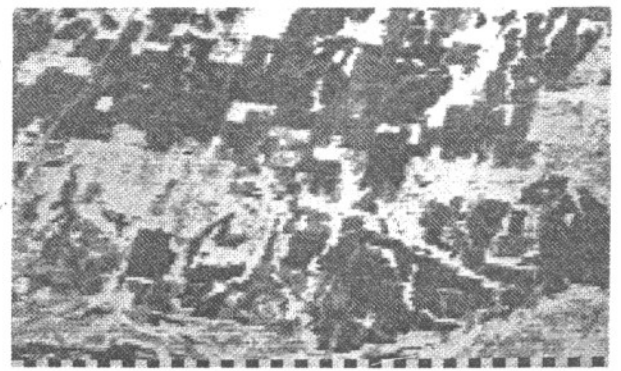
Feature 2, Biophase 1, Greenstuff, SS No. 1172



Feature 6, Biophase 2, Greenstuff, SS No. 1172



Feature 10, Biophase 3, Greenstuff, SS No. 1172

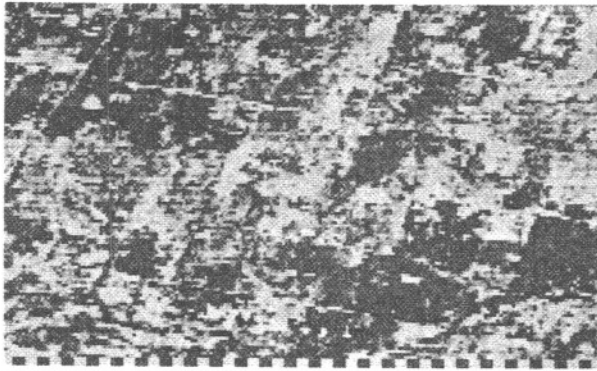


Feature 14, Biophase 4, Greenstuff, SS No. 1172

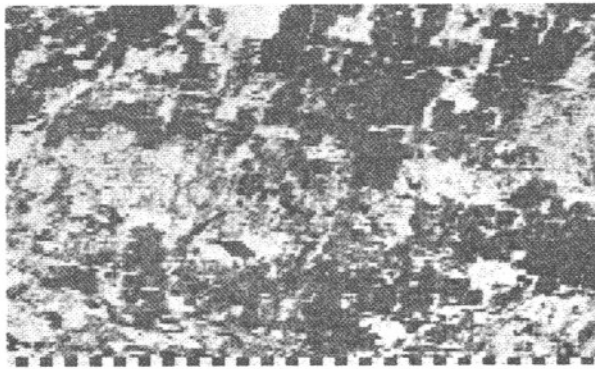
Figure 6. Time Progression of Greenstuff Feature



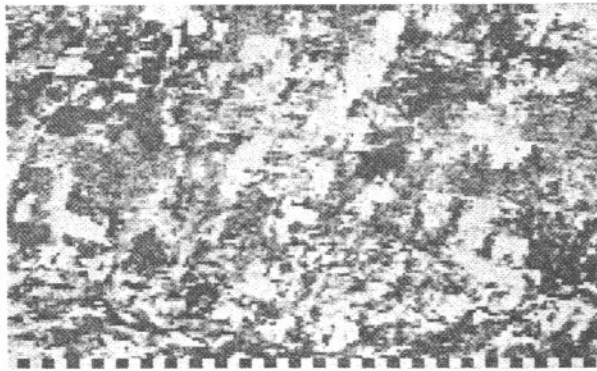
Feature 1, Biophase 1, Brightness, SS No. 1172



Feature 5, Biophase 2, Brightness, SS No. 1172

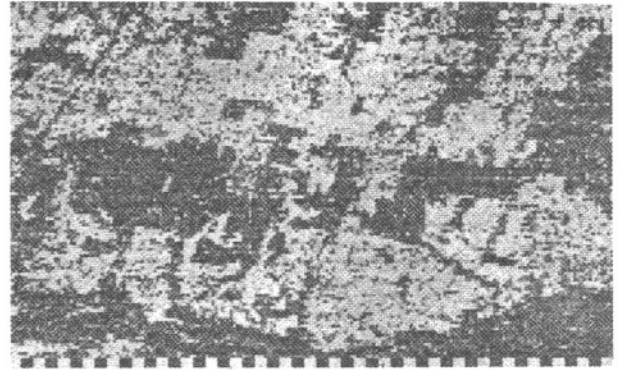


Feature 9, Biophase 3, Brightness, SS No. 1172

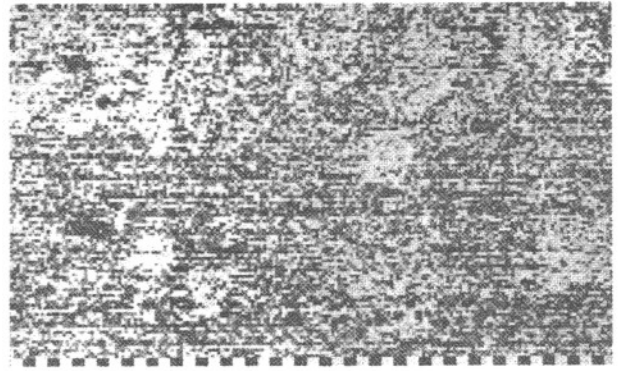


Feature 13, Biophase 4, Brightness, SS No. 1172

Figure 7. Time Progression of Brightness Feature



Feature 15, Biophase 4, Yellow Stuff, SS No. 1172



Feature 16, Biophase 4, Non-such, SS No. 1172

Figure 8. Samples of Yellow-Stuff and Non-Such Features

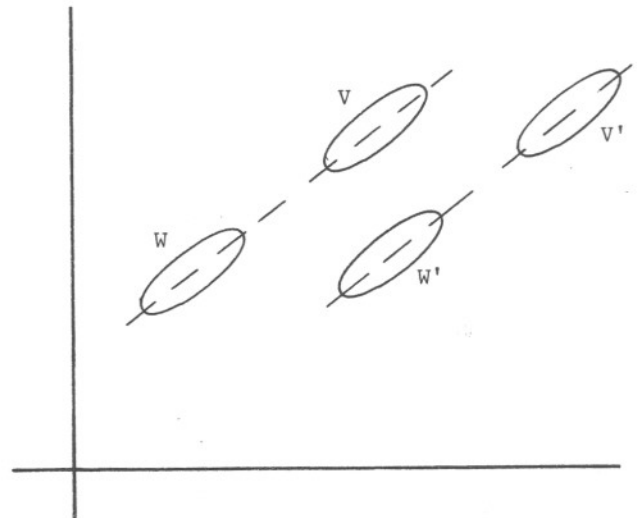


Figure 9. Hypothetical Example of Haze Effect

Table 1. Summary of Various Vectors as Seen by LANDSAT, % Effective Reflectance.  $\mu_s$  is the mean vector of soils.  $V_1$  through  $V_4$  are principal components whose amplitudes are given as  $\sqrt{\lambda}$ .

	CH1	CH2	CH3	CH4	$\sqrt{\lambda}$
$\mu_s$	15.57	21.83	25.55	31.14	48.389
$V_1$	14.22	17.36	18.981	20.23	35.681
* $V_2$	4.23	.018	-2.03	-2.16	5.165
$V_3$	-.57	2.076	-1.54	1.30	2.949
$V_4$	-1.35	.166	.581	-.1408	1.486

#### REFERENCES

- Henderson, R.G., G.S. Thomas, and R.F. Nalepka, Methods of Extending Signatures and Training Without Ground Information, Appendix 3, 109600-16-F, Environmental Research Institute of Michigan, May 1975.
- Suits, G.H., The Calculation of the Directional Reflectance of a Vegetative Canopy, Remote Sensing of Environment, Vol. 2, 1972, pp. 117-125.
- Condit, H.R., The Spectral Reflectance of American Soils, Photogrammetric Engineering, Vol. 36, p. 955, September 1970.
- Condit, H.R., Private Communication.
- Johnson, F., CITARS Vol. 8, Data Processing at the Earth Observations Division, Lyndon B. Johnson Space Center, Part 5, Fayette County, Illinois Supplement: Graphic Study of Corn and Soybean Data. Report Number JSC 09391, December 1975.
- Malila, W.A. and R.C. Cicone, Empirical and Simulation Model Analysis of LANDSAT Signature Variability, Proc. of Third Symposium on Machine Processing of Remotely Sensed Data, West Lafayette, Indiana, June 1976.
- Colwell, J.E. and G.H. Suits, Yield Prediction by Analysis of Multispectral Scanner Data, 109600-17-F, Environmental Research Institute of Michigan, Ann Arbor, May 1975.
- Erickson, Jon D. and Richard F. Nalepka, PROCAMS: A Second Generating Multispectral-Multitemporal Data Processing System for Agricultural Mensuration, Proceedings of the Symposium on Machine Processing of Remotely Sensed Data, West Lafayette, Indiana, June 1976.
- Lambeck, P.F. and D.P. Rice, Signature Extension Via Transformations of Cluster Statistics, Environmental Research Institute of Michigan, Ann Arbor, (to be published).